ACS OMEGA

Open Access

http://pubs.acs.org/journal/acsodf

Article

Performance and Emission Analysis of Biodiesel Blends in a Low Heat Rejection Engine with an Antioxidant Additive: An Experimental Study

Elumalai Perumal Venkatesan,* Silambarasan Rajendran,* Manickam Murugan, Sreenivasa Reddy Medapati, Keerty Venkata Sri Ramachandra Murthy, Mamdooh Alwetaishi, Sher Afghan Khan, and Chanduveetil Ahamed Saleel

Cite This: *ACS Omega* 2023, 8, 36686−36699

Read Online

ACCESS | Metrics & More | Article Recommendations

ABSTRACT: The rapid depletion of crude oil and environmental degradation necessitate the search for alternative fuel sources for internal combustion engines. Biodiesel is a promising alternative fuel for compression ignition (CI) engines due to its heat content and combustion properties. Biodiesel blends are used in various vehicles and equipment, such as cars, trucks, buses, off-road vehicles, and oil furnaces. Biodiesel can reduce emissions from CI engines by up to 75% and improve engine durability due to its high lubricity. However, biodiesel has some drawbacks, including a performance reduction and increased nitrogen oxide emissions. Therefore, this study aims to investigate using environmentally available biodiesel in a low-heat rejection engine and an antioxidant additive to enhance the performance and reduce nitrogen oxide emissions. India currently has several biodiesel sources, including mango seed oil, mahua oil, and pongamia oil, which can be effectively utilized in CI engines by adding L-ascorbic acid. The experimental work involves a single-cylinder 4-stroke water-cooled direct injection CI engine with a power output of 5.2 kW. The engine's cylinder head, piston head, and valves are coated with lanthanum oxide using the plasma spray coating technique, with a thickness of 0.5 mm. The coated and uncoated engines are tested with different proportions of mahua oil, mango seed oil, and pongamia oil. The results show that the engine's performance is significantly improved compared to the baseline engine at all loads. Additionally, these biodiesels exhibit a notable reduction in nitrogen oxide emissions when combined with L-ascorbic acid.

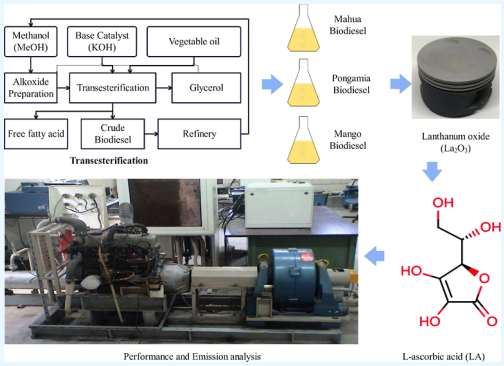

1. INTRODUCTION

Depletion of fossil fuel, the ever-increasing demand for fuel, and severe environmental issues lead us to go from alternate fuel to compression ignition (CI) engines. The application of pongamia biodiesel in a CI engine affects performance and emission characteristics. The experiments are conducted with 5, 10, and 15% blends of pongamia biodiesel as a substitute for diesel fuel. The 10% blend has the optimum brake-specific fuel consumption (BSFC) and brake thermal efficiency (BTE).[1] The performance and emission characteristics of the mahua methyl ester using the additive. They used neat diesel and neat mahua biodiesel and mixed them with 5, 10, and 15% dimethyl carbonate as additives. The BTE of neat mahua biodiesel is lower than that of diesel, and adding additives results in a slight increase in BTE with an increase in the proportion of mahua biodiesel. Furthermore, biodiesel has lower CO and HC emissions than diesel due to its higher oxygen content and additive addition.[2] The performance and emission behavior of the methyl ester mango seed oil in a diesel engine. The physical properties of MEMSO are like those of diesel, which shows its suitability as fuel in CI engines. The CO emission of the MEMSO blend ratio of 75% is lower than that of diesel but higher for neat MEMSO. All the blends' BTE, smoke, and HC emissions are lower than diesel at all load conditions.[3] Performance and emission study of mahua oil ethyl ester (MOEE) in a DI diesel engine.[4] They have found that the BTE of MOEE is slightly lower, whereas the SFC is higher than diesel's due to its lower calorific value.[5] The performance and emission characteristics of different blends of mahua methyl ester with diesel in a multicylinder turbocharged diesel engine. There is an increase in BSFC and a reduction in BTE, with an increase in the proportion of biodiesel. The HC and CO

Received: April 21, 2023
Accepted: September 19, 2023
Published: September 29, 2023

emissions of the mahua methyl blends are lower than those of diesel.[6]

The performance and emission characteristics of the mullite-coated low heat rejection (LHR) engine. They coated the piston crown, cylinder head, and valves with a 0.5 mm thickness of $3Al_2O_3{\cdot}2SiO_2$ (mullite) (Al_2O_3 is 60%, SiO_2 is 40%) over a 150 μm thickness of NiCrAlY bond coat. The SFC is decreased by 2.18% for the LHR engine with a turbocharger compared to a standard engine full load. There is a 2% increase of exhaust gas temperature (EGT) and a 20.64% increase in NOx emissions for LHR engines at full load.[7] The effect of TBC on turbocharged diesel engines was compared to that of a standard diesel engine. The TBC engine has a lower BSFC and higher BTE due to the increase in the combustion chamber temperature. They found a 3−27% increase in the energy available in the exhaust gas in TBC engines, which can be utilized by turbochargers.[8] The effect of TBC coating on the performance and emission characteristics of a diesel engine. The engine cylinder heads, valves, and pistons are coated with 0.15 mm of a nickel−chrome−aluminum bond coat and 0.35 mm of YSZ. The coated engine has reduced the ignition delay (ID) period and affected BSFC negatively. It is seen that more oxygen content of biodiesel increases the NOx emission in the exhaust.[9] The LHR engine's combustion, performance, and emission characteristics are coated with partially stabilized zirconia using jatropha seed oil biodiesel. It is found that there is a higher peak pressure for the LHR engine due to earlier heat release. It is also found that the mean temperature of the LHR engine fueled with biodiesel is increased by about 5, 13, and 18% compared to that of LHR with diesel.[10]

The combustion, performance, and emission characteristics of LHR engines operating on various biodiesel and vegetable oils.[11] They concluded that the LHR engine performance characteristics are better in terms of power, fuel consumption, and thermal efficiency for all the fuels. LHR engine emission characteristics have been reported to have improved significantly except NOx for all fuels due to higher combustion chamber temperatures.[12] Coated diesel engine piston with titanium oxide of 0.5 mm by plasma spray coating method and analyzed the performance and combustion characteristics of B20 and B100 of PME. The heat release rate (HRR) of the B100-coated engine is higher due to the higher combustion temperature. It is found that there is an improvement in BTE and a decrease in BSFC for coated engines. The exhaust emissions like CO and HC are decreased, and the NOx emission is increased by 15% with the coated engine.[13]

The effect of antioxidants on NOx emissions from the jatropha biodiesel-fueled diesel engine. The antioxidants such as L-ascorbic acid (vitamin C), a tocopherol acetate (vitamin E), butylated hydroxytoluene (BHT), *p*-phenylenediamine (PPDA), and ethylenediamine (EDA) are mixed about 0.025% by volume with biodiesel. The result shows a reduction of NOx significantly at all loads for all antioxidant additives.[14] The effect of an antioxidant additive on NOx emissions from a mango oil biodiesel-fueled engine. The diethyl amine (DEA), pyridoxine hydrochloride (PHC), and *tert* butyl hydroquinone (TBHQ) are used for the tests. The performance and emission characteristics were evaluated at different concentrations of antioxidant additive, that is, 100, 250, 500, and 1000 ppm with the B20 blend. It is seen that antioxidants with biodiesel mixtures reduced the NOx emissions considerably.[15] The effect of *N*,*N*′-diphenyl-1,4-phenylenediamine (DPPD), *N*-phenyl-1,4-phenylenediamine (NPPD), and 2-ethylhexyl nitrate (EHN) on the performance and emission behavior of the 20% blend of calophyllum ininophyllum biodiesel with diesel. Adding 1000 ppm of antioxidants with B20 blend has improved the blend's oxidation stability without affecting the fuel's properties. It is found that DPPD is a better additive to improve the oxidation stability. Further, the B20 has less BTE and higher BSFC compared to diesel. It is seen that additives have a positive effect in reducing the NOx emissions at the expense of an increase in CO and HC emissions.[16] The oxidation stability and exhaust emissions of 20% blend of moringa oleifera biodiesel with aromatic amine antioxidants. They used 2000 ppm of DPPD and NPPD with B20 fuel. The DPPD and NPPD have increased the oxidation stability of the B20 blend up to the induction period of 34.5 and 18.4 h, respectively.[17]

The objective of the present work is to explore the possibility of renewable fuels, which can perform better than diesel fuel in terms of performance, combustion, and emission characteristics. Renewable fuels such as mango seed, mahua, and pongamia biodiesels are used as diesel fuel substitutes in the present work. These biodiesels are widely used in CI engines and have the drawback of lower performance and higher NO emissions.[18] These problems can be prevented by providing the LHR mode in the CI engine and adding additives with biodiesel. The LHR engine will enhance combustion, leading to improved performance, and adding additives in biodiesel will improve biodiesel properties and reduce NOx emissions significantly.[19,20] Hence, an attempt is made to study the effect of mango seed, mahua, and pongamia biodiesels with LHR engine and additives with different proportions on the engine performance, combustion, and emission characteristics in a single-cylinder direct injection CI engine.[21]

2. EXPERIMENTAL METHODOLOGIES

The biodiesel is produced from raw biofuel production and fatty acids and converted into biodiesel by the trans-esterification. Energy and environmental production agencies have limited the biodiesel feedstock to nonedible sources due to the possibility of demand for edible oils. The researchers in India suggested that biodiesel production, such as jatropha oil, *Pongamia pinnata* oil, mahua oil, *Nerium* oil, neem oil, calophyllum inophyllum oil, rubber seed oil, cashew nutshell liquid, and mango seed oil, can be used in CI engines. In this present investigation, mango seed oil, mahua oil, and pongamia oil are chosen as the feedstock due to their availability and relatively being cheaper than other sources. Physical properties of these three biodiesels are relatively closer to those of diesel fuel.[22]

2.1. Mahua. *Madhuca longifolia*, also known as mahua, is an Indian tropical tree found predominantly in the Indian plains and forests. It belongs to the family Sapotaceae and is characterized by its fast growth, reaching heights of approximately 20 m. The tree exhibits evergreen or semievergreen foliage. Each tree can yield between 20 and 200 kg of seeds annually, depending on its maturity. In Figure 1 and 2, you can see photographs of the Mahua seed and fruit. The oil extraction involves using a mechanical crusher to extract oil from sun-dried seeds. Mahua oil cakes have found application as fertilizers in the agricultural sector. The oil itself is a sunset yellow color.

2.2. Pongamia. Millettia pinnata, also known as *P. pinnata*, is an evergreen tree commonly found in the rainforests of Asia

https://doi.org/10.1021/acsomega.3c02742
ACS Omega 2023, 8, 36686−36699

Figure 1. Mahua fruit with seed.

Figure 2. Mahua seed.

and has been cultivated worldwide. It thrives in regions with moderate to high humidity. The tree produces seeds with an average yield ranging from 10 to 50 kg per tree per year, depending on maturity. The weight of each seed is approximately 1.1−1.8 g. In Figure 3, you can see a

Figure 3. Pongamia pod and seed.

photographic view of the *P. pinnata* pod and seed. The tree starts yielding pods around the fifth year, gradually increasing until the twelfth year, when it stabilizes. Pongamia oil is extracted from the seeds using mechanical expeller, cold pressing, or solvent extraction methods. The oil has a yellowish-orange to brown color.

2.3. Mango. *Mangifera indica*, commonly known as the mango tree, is a tall tree that can reach heights of 15−30 m. It is widely cultivated in various regions of Tamil Nadu, India, primarily for its fruit. Mango trees thrive in well-drained sandy loam soil and prefer a pH ranging from 5.2 to 7.5 for optimal growth. The mango fruit typically contains a single seed stone at the center, which accounts for approximately 10% of the total fruit weight. Figure 4 provides a photographic view of

Figure 4. Mango seed stone and kernel.

mango seed stones and the mango kernel. The stones are dried, and the hull surrounding the kernel is removed manually or mechanically. Mango seed oil can be extracted from thoroughly dried kernels by using a mechanical expeller. The oil is soft yellow and typically exists in a semisolid state at room temperature, with a melting point of around 30 °C.

3. PROPERTIES OF TEST FUELS

Table 1 shows the comparative study of the properties of mango seed oil, mahua oil, and pongamia oil before

Table 1. Properties of Raw Pongamia Oil, Mango Seed Oil, Mahua Oil, and Diesel

Properties	pongamia oil	mango seed oil	mahua oil	diesel
kinematic viscosity at 40 °C (m^2/s)	40.2	20.97	68	2.9
calorific value (kJ/kg)	37,500	41,803	38,957	42,700
density@15 °C (kg/m^3)	924	917	918	840
cetane index	38	50.6	34	49
flash point (°C)	225	298	238	54
fire point (°C)	256	315	244	64

transesterification. It is seen from the table that some properties of the mango seed oil, mahua oil, and pongamia deviate from standard diesel properties. Viscosity is especially higher for all oils than that of diesel fuel. Further, vegetable oil's density, flash, and fire point are higher than diesel fuel's. To improve the above properties, transesterification is required before use in the CI engine.

3.1. Transesterification. The viscosity of vegetable oil is very high compared to diesel. In a CI engine, fuel is injected into a combustion chamber with a very high pressure at the end of the compression stroke. The fuel is atomized and mixes with air. Raw vegetable oil used in CI engines will lead to poor atomization, followed by poor combustion and higher exhaust emission levels due to its higher viscosity. Therefore, the raw vegetable oil viscosity must be reduced by using transesterification and pyrolysis methods. Among the various methods used to reduce the viscosity of vegetable oil, the transesterification method brings the viscosity of vegetables much closer to that of diesel fuel, and the biodiesel yield will be 60−90%. Transesterification is a chemical reaction where vegetable oil triglyceride reacts with alcohol in a NaOH or KOH catalyst to produce alkyl esters with glycerol as a byproduct. The chemical reaction in the transesterification is shown in Figure 5.

3.2. Properties of Test Fuels (after Transesterification). Figure 6 shows the flow diagram for biodiesel

https://doi.org/10.1021/acsomega.3c02742
ACS Omega 2023, 8, 36686−36699

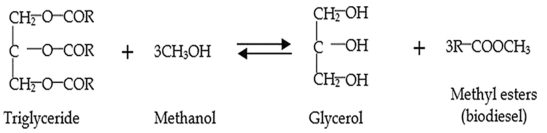

Figure 5. Chemical reaction in transesterification.

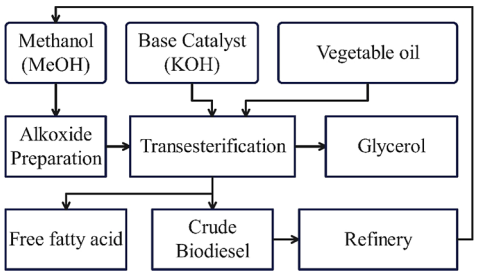

Figure 6. Transesterification process flowchart.

production; the physical properties of diesel, mango seed methyl ester (100%), mahua methyl ester (100%), and pongamia methyl ester (100%) are shown in Table 2. The properties of these fuels are measured using ASTM D 6751, a prescribed method for testing of fuel properties.

Density of MEPO is higher than the EN14214 limit of 0.86−0.9, and the densities of other biodiesels are within the limits and are closer to diesel. The kinematic viscosity of MEMSO is lower than that of another biodiesel and is much closer to that of the diesel. Cetane numbers of all the biodiesels are higher than those of the diesel, which shows a higher self-ignition temperature. Properties of diesel, mango seed methyl ester (20%), mahua methyl ester (20%), and pongamia methyl ester (20%) are shown in Table 3.

Investigating 20 and 100% biodiesel blends in this study can be attributed to various factors. First is the practicality of these blends. A 20% biodiesel blend, commonly called B20, is widely used in many regions and is readily available in the market. It has been extensively tested and works effectively in existing diesel engines without requiring significant modifications. By studying the performance and emission characteristics of B20, researchers can gain valuable insights into its practical application and evaluate its potential as a viable alternative fuel. Regulatory requirements may also play a role in the selection of these specific blends. In certain countries or regions, regulations or standards that mandate the use of a minimum biodiesel blend, such as B20, in certain applications or for achieving specific emission reduction targets may be in place. Therefore, conducting investigations on B20 allows researchers to assess compliance with these regulations and understand the impact of such blends on the engine performance and emissions.

On the other hand, studying the use of 100% biodiesel (B100) is crucial to exploring biodiesel's full potential as a standalone fuel. It allows researchers to assess the performance and emission characteristics when using biodiesel exclusively, without any petroleum-based diesel fuel. Understanding the behavior of B100 provides insight into the maximum potential of biodiesel as a sustainable and renewable fuel source for diesel engines. This investigation covers a range of biodiesel concentrations by focusing on 20 and 100% biodiesel blends. It allows for a comprehensive evaluation of their effects on engine performance, emissions, and compliance with regulatory requirements.

3.3. Selection of Coating Material. Materials with low thermal conductivity and high thermal stability are suitable for coating. The literature review shows that ceramic materials such as zirconia, alumina, magnesia, silicon carbide, and rare earth metals such as lanthanum oxide are considered in much research for coating on the combustion chamber component. It is found from the literature review; very minimal work has been conducted in using lanthanum oxide as a coating material in engine components.

Lanthanum oxide (La_2O_3) is a rare earth element with lanthanum and oxygen. Lanthanum oxide is an odorless, white solid that is insoluble in water but is insoluble in dilute acid. La_2O_3 is hygroscopic; lanthanum oxide absorbs moisture under the atmosphere and converts it to lanthanum hydroxide. La_2O_3 has a low thermal conductivity and higher thermal expansion, equal to that of metals. Because of its higher thermal expansion coefficient, it is selected as a coating material for the CI engine combustion chamber in the present investigation. The properties of lanthanum oxide are given in Table 4.

3.4. Selection of an Antioxidant Additive. An antioxidant is a molecule that inhibits the oxidation of other molecules. Oxidation can produce free radicals, which can start the chain of oxidation reactions in fuels. Antioxidants interrupt chain reactions by preventing the formation of hydroperoxides, peroxides, soluble gums, or insoluble particulates. These are often reducing agents, such as hindered phenols, aromatic amines, and diamines, or mixtures of aromatic, phenylene, and alkyl phenols. Antioxidant additives like L-ascorbic acid, butylated hydroxyl anisole (BHA), TBHQ, BHT, and EHN serve the dual purpose of increasing the oxidation stability of biodiesel and suppressing the NOx emissions.

Based on the electronegativities, L-ascorbic acid (LA) is more suitable for forming complex bonds between free radicals and antioxidant radicals to stabilize the ester chain. The biodiesel blend storage ability and aging effect can also be treated with LA antioxidant. In the present work, based on the suitability, LA is selected to suppress the NOx emissions. The physiochemical property of LA is given in the Table 5.

Table 2. Properties of Test Fuels (B100)

properties	diesel	MEMSO	MEMO	MEPO
density@15 °C in (kg/m^3)	0.8344	0.85	0.8835	0.95
kinematic viscosity@40 °C (m^2/s)	3.07	3.26	3.46	3.86
flash point (°C)	60	90	150	226
fire point (°C)	69	95	161	253
calorific value (kJ/kg)	44,125	42,095	39,292	36,000
cetane number	46	52	54	48

https://doi.org/10.1021/acsomega.3c02742
ACS Omega 2023, 8, 36686−36699

Table 3. Properties of Test Fuels (B20)

Properties	diesel	MEMSO	MEMO	MEPO
density@15 °C in (kg/m^3)	0.8344	0.85	0.84	0.87
kinematic viscosity@40 °C (m^2/s)	3.07	3.12	3.21	3.48
flash point (°C)	60	85	120	185
fire point (°C)	69	88	152	235
calorific value (kJ/kg)	44,125	42,895	39,992	37,400
cetane number	46	50	51	47

Table 4. Properties of Lanthanum Oxide

chemical formula	La_2O_3
molar mass	325.809 g/mol
Appearance	white powder, hygroscopic
thermal expansion coefficient	573−1573 C
Density	6.51 g/cm^3, solid
melting point	2315 °C
boiling point	4200 C
solubility in water	insoluble
band gap	4.3 eV

Table 5. Properties of L-Ascorbic Acid

chemical structure	
CAS number	50-81-7
minimum assay (%)	99
molecular formula	C_6H_8O
molar mass (g mol^{-1})	176.12
Appearance	white or light yellow solid
molecular weight (g/mol)	176.13
melting point (°C)	192−192
density (g/cm^3)	1.65

4. EXPERIMENTAL SETUP

Load testing has been carried out in a single-cylinder CI engine attached to an eddy current dynamometer to vary the load. The load was measured by a load cell attached to the dynamometer arm. The setup has the provision to measure the fuel flow rate and air flow rate into the engine. The setup is provided to measure and control the coolant flow rate. Crank angle encoder is used to measure the piston position, and PCB piezo electronics make the pressure transducer used to measure the in-cylinder gas pressure. The AVL 444 digas analyzer and AVL smoke meter measure the engine exhaust emissions. The line diagram of the experimental setup with the necessary equipment is shown in Figure 7.

The engine can run with neat diesel at a constant speed of 1500 rpm to attain steady state condition. The exhaust gas analyzer and smoke meter are switched on quite early to stabilize all of their systems before the experiment begins. The above experimental procedure is followed for conducting all experiments. The details of the experiments for the present investigation are as follows:

1. After completing the experiments with neat diesel, the same experimental procedure is repeated with a B20 blend of the mango seed oil methyl ester (MEMSO). The experiments and similar observations are repeated with the B100 for MEMSO. After completing the experiment with the MEMSO biodiesel, the engine is allowed to run for about half an hour with diesel to eliminate interference from the previous biodiesel fuel.
2. The experiments for mahua methyl ester (MEMO) and pongamia methyl ester (MEPO) for 20 and 100% proportions are conducted similarly.
3. The experiment for B20 of MEMSO, MEMO, and MEPO in a lanthanum oxide-coated LHR engine is conducted.
4. Different proportions of LA were added with diesel, and experiments were conducted in a conventional engine to find the optimum proportion of LA.
5. Experiments are conducted with different proportions of LA with B20 of three biodiesel blends in conventional engines.
6. 200 mg LA with 20% of three biodiesel blends in the LHR engine.

Figure 7. Photographic view of the experimental setup.

5. RESULTS AND DISCUSSION

5.1. Biodiesel Blends with Diesel. Biodiesels such as methyl esters of mango seed oil (MEMSO), pongamia oil (MEPO), and mahua oil (MEMO) are blended with diesel by 20 and 100% proportions. The experiments for different MEMSO, MEPO, and MEMO proportions are conducted in a single-cylinder DI CI engine at a constant speed of 1500 rpm. The observations for fuel consumption, EGT, and emission parameters, such as CO, HC, NOx, and smoke, are made. Based on the observations, BSFC and BTE are calculated, and the graphs are plotted for BSFC, BTE, CO, HC, NOx, smoke, and EGT with engine brake power. A detailed result and discussion of individual parameters are given below.

5.1.1. Different Biodiesel with 20 and 100% Proportions. The 20 and 100% proportions of MEMSO, MEPO, and MEMO methyl ester are used in the experiments, and various parameters such as the time taken for fuel consumption, EGT, CO, HC, NOx, and smoke are observed. The graphs are plotted for the variation of BSFC, BTE, EGT, emissions of carbon monoxide (CO), hydrocarbon (HC), oxides of nitrogen (NOx), and smoke concerning brake power (BP).

5.1.1.1. Brake-Specific Fuel Consumption. The deviation of BSFC concerning BP for 20 and 100% proportions of MEMSO, MEPO, MEMO, and diesel is shown in Figure 8. It is seen that different proportions of biodiesel have higher

https://doi.org/10.1021/acsomega.3c02742
ACS Omega 2023, 8, 36686−36699

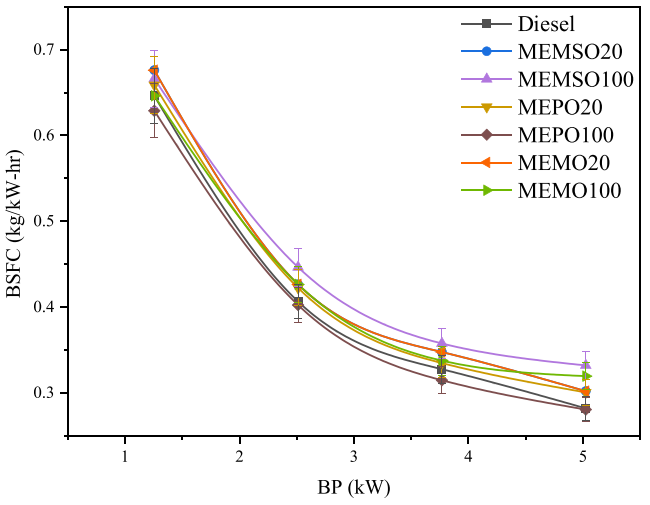

Figure 8. Deviation of BSFC vs BP for 20 and 100% blends of three biodiesels.

BSFC than that diesel. It is due to the blends' high viscosity and poor volatility, which result in poor atomization and mixture formation. The BSFC for 100% biodiesel is higher compared to that of 20% proportion biodiesel. It is because 100% biodiesel has a lower heating value and requires excess fuel to maintain the same power output of the engine. Among the different proportions of biodiesel, MEMSO20 showed lower BSFC than other blends, which is very close to diesel fuel.

5.1.1.2. Brake Thermal Efficiency. The deviation of BTE with respect to BP for 20 and 100% proportions of MEMSO, MEPO, MEMO, and diesel is shown in Figure 9. It is evident

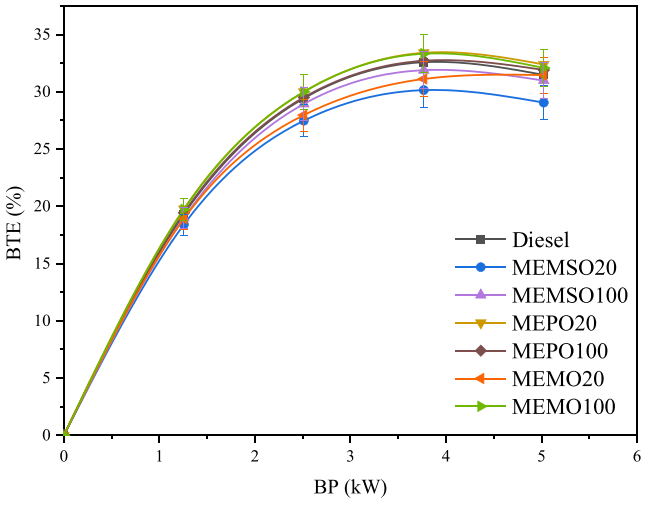

Figure 9. Deviation of BTE vs BP for 20 and 100% blends of three biodiesels.

from the graph that diesel showed higher BTE. This may be due to a higher calorific value and lower density of diesel. Among the different proportions, MEMSO20 showed higher BTE but lower than diesel. It is mainly because of CV, cetane number, and density, which are almost equal to diesel fuel. It is also seen from the graph that 100% blends of three biodiesel indicated lower BTE than 20% blends. This may be due to the 20% blend having superior properties to 100% biodiesel.25 diesel.

5.1.1.3. Exhaust Gas Temperature. The deviation of EGT concerning BP for 20 and 100% blends of MEMSO, MEPO, MEMO, and diesel is shown in Figure 10. The EGT indicates

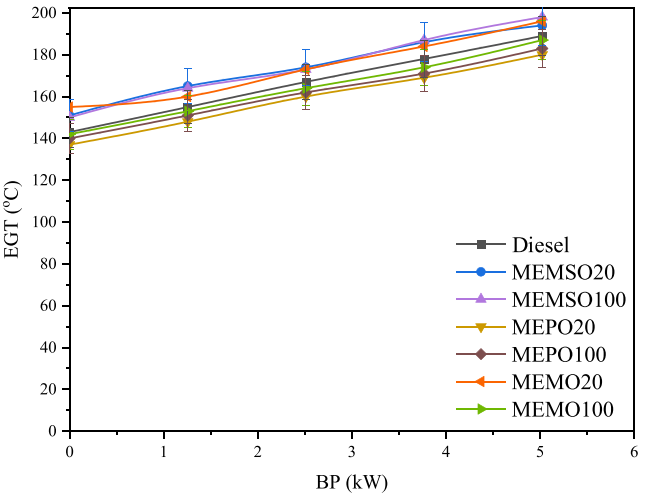

Figure 10. Deviation of EGT vs BP for 20 and 100% blends of three biodiesels.

the heating capacity of the fuel used, and 1/third of the heat comes out as EGT. It is seen that EGT increases with the proportions of biodiesel at all loads. It is observed from the graph that MEPO100 showed a higher EGT than others at all loads. Since MEPO has a lower CV and higher density, incomplete combustion leads to an increase in EGT. It is also observed that MEMSO20 showed lower EGT among the blends and a slight increase compared to diesel. It is because MEMSO20 has excess oxygen, higher CV, and a lower density than other blends.

5.1.1.4. Carbon Monoxide Emission. The deviation of the CO concerning BP for 20 and 100% blends of MEMSO, MEPO MEMO, and diesel is shown in Figure 11. It is seen from Figure 11 that MEMSO20 has lower CO emissions and diesel has higher emissions at all loads. This shows biodiesel contains more oxygen, leading to complete combustion.[23] It indicates that the combustion efficiency improved, and the

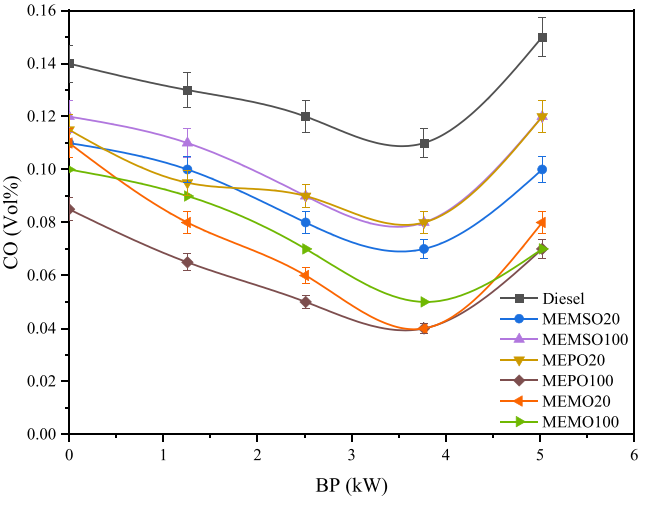

Figure 11. Deviation of CO emission vs BP for 20 and 100% blends of three biodiesels.

https://doi.org/10.1021/acsomega.3c02742
ACS Omega 2023, 8, 36686−36699

level of CO emission was reduced compared to diesel. The reason for the reduction of CO for MEMSO20 is the presence of excess oxygen and the effective combustion of biodiesel.

5.1.1.5. Hydrocarbon Emission. The deviation of HC concerning BP for 20 and 100% blends of MEMSO, MEPO, MEMO, and diesel is shown in Figure 12. The HC emission

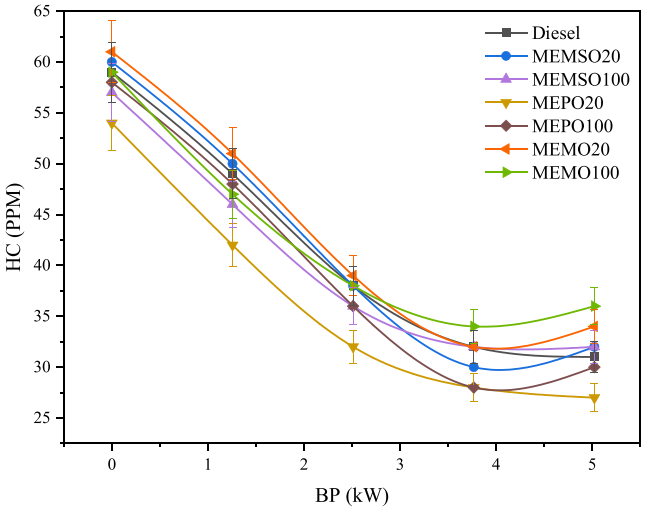

Figure 12. Deviation of HC emission vs BP for 20 and 100% blends of three biodiesels.

for MEMSO20 is lower than that of other blend proportions and diesel at all load conditions. Since MEMSO20 has a higher heating value and leads to effective combustion.[24] Among the different fuels, diesel showed higher HC emissions, which may be due to the diesel's lack of oxygen, leading to poor atomization. It is seen that MEPO100 shows higher HC emissions since it has a lower heating value than others.

5.1.1.6. Oxides of Nitrogen Emission. The deviation of NOx emission concerning BP for 20 and 100% blends of MEMSO, MEPO, MEMO, and diesel is shown in Figure 13. The NOx formation is based on the oxygen content of the fuel, combustion flame temperature, and reaction time in the combustion chamber. The NOx emission of biodiesel blends is higher than that of diesel fuel and increases with load. It is due

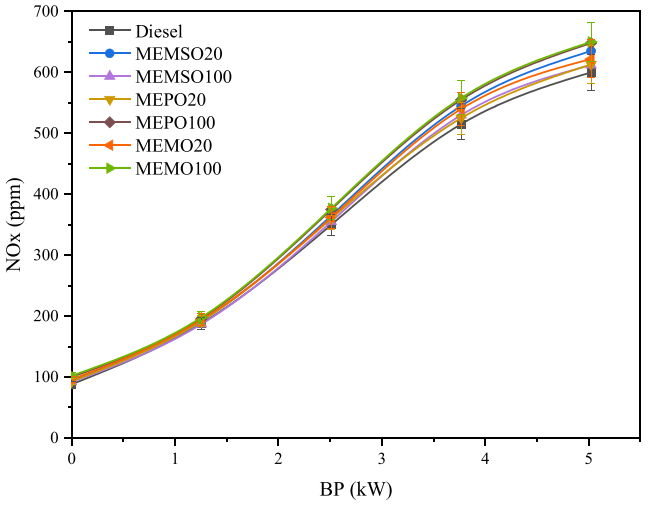

Figure 13. Deviation of NOx emission vs BP for 20 and 100% blends of three biodiesels.

to the higher temperature of combustion and the presence of oxygen in the biodiesel, causing higher NOx than that of diesel fuel.[25] MEMSO has NOx emissions lower than those of other blends among the different biodiesel blends.

5.1.1.7. Smoke Opacity. The deviation of smoke opacity emission concerning BP for 20 and 100% blends of MEMSO, MEPO, and MEMO and diesel is shown in Figure 14. The

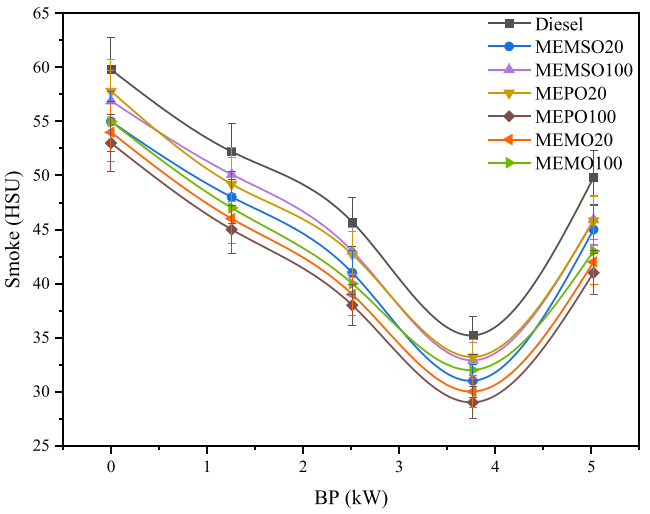

Figure 14. Deviation of smoke opacity vs BP for 20 and 100% blends of three biodiesels.

smoke is produced more in the diffusive combustion phase. Since oxygenated fuel blends such as MEMSO, MEPO, and MEMO lead to an improvement in diffusive combustion. It is seen from the graph that the smoke opacity is lower for MEMSO20 at all loads. This is because of the higher heating value and excess oxygen in the fuel, which makes better combustion and reduces smoke opacity.[26] Among the biodiesel blends, MEPO 100 showed higher smoke opacity since it has a lower heating value and cetane number, which causes poor combustion and increases smoke opacity. Further, higher density at 100% blend leads to poor atomization. The diesel showed higher smoke opacity due to the presence of aromatic compounds compared to that of biodiesel.[27]

5.2. Biodiesels with 20% Blend in LHR Engine. It is noted from the previous experiments that 20% proportions of three biodiesels showed better results than other blends. The BTE of all biodiesel blends is lower when compared with that of diesel. To improve the efficiency, the engine is converted into the LHR mode, 20% proportions of three biodiesel are used as a fuel, and the experiments are conducted. The performance and emission parameters are observed, and graphs are plotted with BP for BSFC, BTE, CO, HC, NOx, EGT, and smoke opacity.

5.2.1. Brake-Specific Fuel Consumption. The deviation of BSFC concerning BP for 20% blends of three biodiesel in the LHR engine is shown in Figure 15. It can be found from Figure 15 that the BSFC for diesel is lower than that of other blends. This is due to the LHR engine's higher heating value, lower viscosity, and fuel density. Among the three biodiesels, MEMSO20 showed lower BSFC than that of others. This is due to the increased cylinder temperature because of the thermal coating, which resulted in less fuel consumption to develop the same power output.[28] Further, the coating at various combustion elements of the engine is believed to

https://doi.org/10.1021/acsomega.3c02742
ACS Omega 2023, 8, 36686−36699

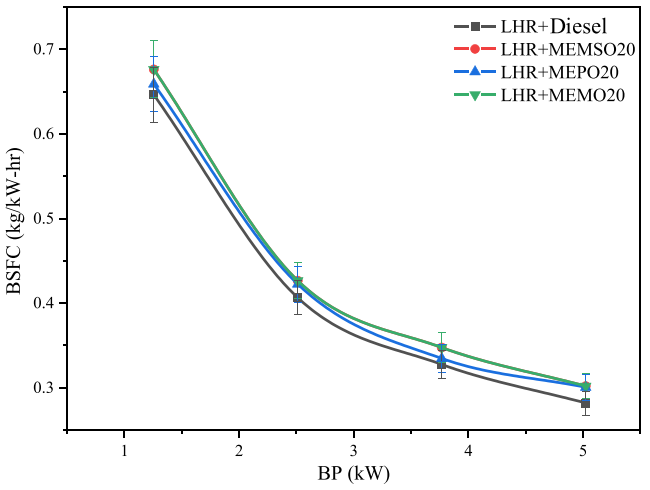

Figure 15. Deviation of BSFC vs BP for 20% blends in the LHR engine.

increase the cylinder gas temperature, contributing to the higher vaporization rate and reducing fuel consumption.

5.2.2. Brake Thermal Efficiency. The deviation of the BTE concerning BP for 20% blends of three biodiesels is shown in Figure 16. It is found that BTE is higher for diesel in LHR

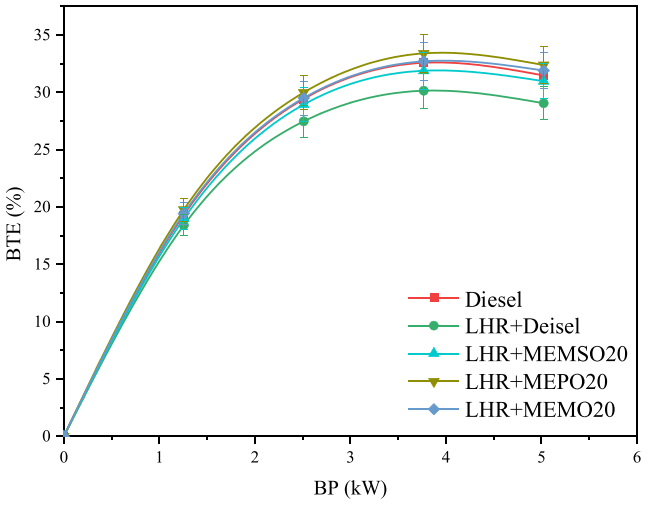

Figure 16. Deviation of BTE vs BP for 20% blends in the LHR engine.

engine. This is because higher combustion chamber temperature makes effective combustion for diesel fuel. The BTE of 20% biodiesel blends is lower than that of diesel, possibly because of the lower calorific values and higher density of biodiesels. Further, it is also found that MEMSO20 has higher BTE among the other biodiesel blends.

5.2.3. Exhaust Gas Temperature. Figure 17 shows the deviation of EGT concerning BP for 20% blends of three biodiesels in the LHR engine. The EGT increases with load for all proportions since the engine operates under LHR. It is observed that diesel has a lower EGT and MEPO20 has a higher one. This is because diesel fuel has better combustion and MEPO has a lower calorific value.[29] It is also observed that all biodiesels have a higher EGT at all loads, and this may be because of higher viscosity and density, which makes higher heat available in the EGT.

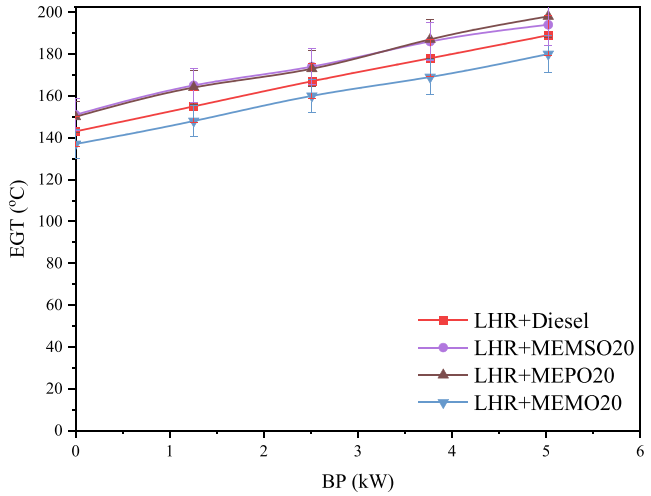

Figure 17. Deviation of EGT vs BP for 20% blends in the LHR engine.

5.2.4. Carbon Monoxide Emission. The deviation of CO concerning BP for 20% blends of three biodiesels in the LHR engine is shown in Figure 18. The CO emission for diesel is

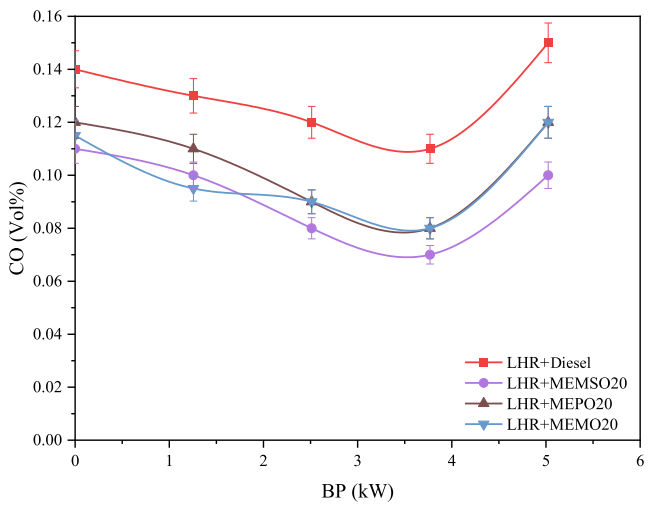

Figure 18. Deviation of CO vs BP for 20% blends in LHR.

higher because more heat generated from the fuel combustion is lost due to impingement on the cylinder wall, leading to incomplete combustion. It was observed that all biodiesel blends showed lower CO emissions than diesel at all loads. Among the various fuels in the LHR engine, MEMSO20 showed a significant reduction of CO than others.[30] This is due to the higher molecular oxygen present in the MEMSO, which makes for better combustion.

5.2.5. Hydrocarbon Emission. Figure 19 shows the deviation of HC concerning BP for 20% blends of three biodiesel in the LHR. The HC emission for MEMSO 20% is lower than that of other biodiesel blends with LHR, and diesel is more at all loads.[31] This is due to a higher oxygen content and higher temperature at the combustion chamber walls of the LHR engine, which cause complete combustion. Further, the LHR engine is desirable to increase the gas temperature and oxidize all the unburnt hydrocarbons. It is seen from the graph that, among the biodiesel blends, MEPO20 showed an

https://doi.org/10.1021/acsomega.3c02742
ACS Omega 2023, 8, 36686−36699

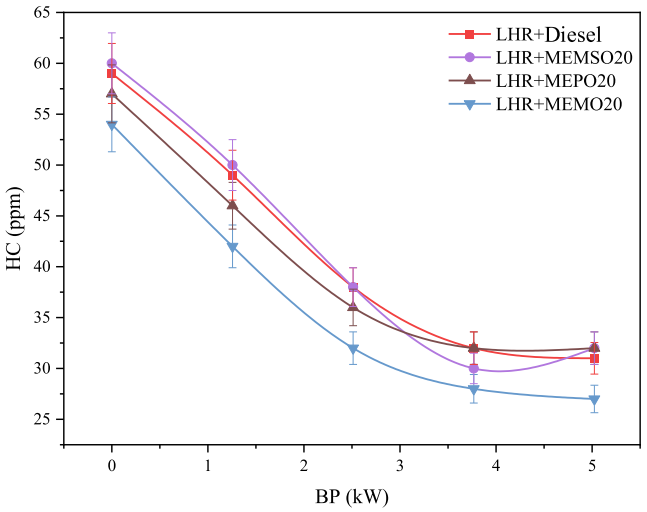

Figure 19. Deviation of HC vs BP for 20% blends in LHR engine.

emission higher than that of the others. This may be due to the inferior properties of MEPO20 compared to other blends.

5.2.6. Oxides of Nitrogen Emission. The deviation of NOx concerning BP for 20% blends of three biodiesels and diesel in the LHR engine is shown in Figure 20. LHR engines have

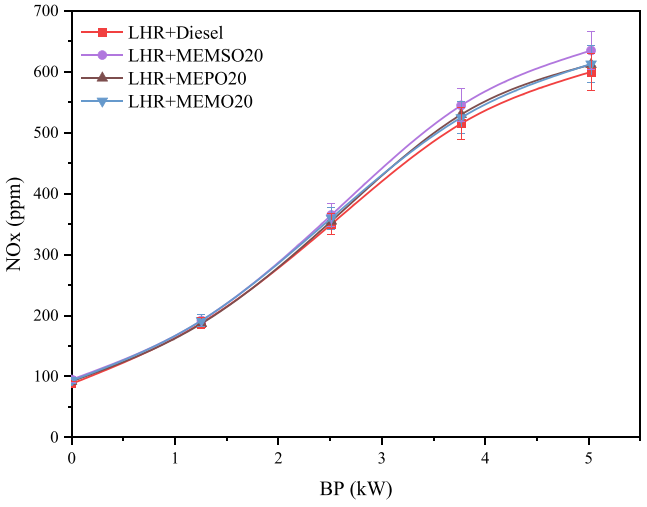

Figure 20. Deviation of NOx vs BP for 20% blends in the LHR engine.

higher NOx emissions than diesel-operated engines at all loads. This is due to the higher combustion chamber temperature and reduced ID in the LHR mode. At maximum load, the NOx emission for MEMSO20 is 649 ppm, which is 15% higher than diesel in LHR.[32] NOx emission is also increased in all blends while operating in the LHR mode. More O_2 content in the biodiesel blends and thermally coated engines increases combustion temperature, thereby increasing NOx emissions.

5.2.7. Smoke Opacity. The deviation of smoke concerning BP for 20% blends of three biodiesels in the LHR engine is shown in Figure 21. The smoke opacity increases with load for all fuels. Among the various fuels operated in LHR engine, MEMSO20 showed more reduction of smoke opacity at all loads. This is due to the higher oxygen content in the MEMSO20 blend and the higher temperature in the combustion chamber in the thermally coated engine.[33] It is

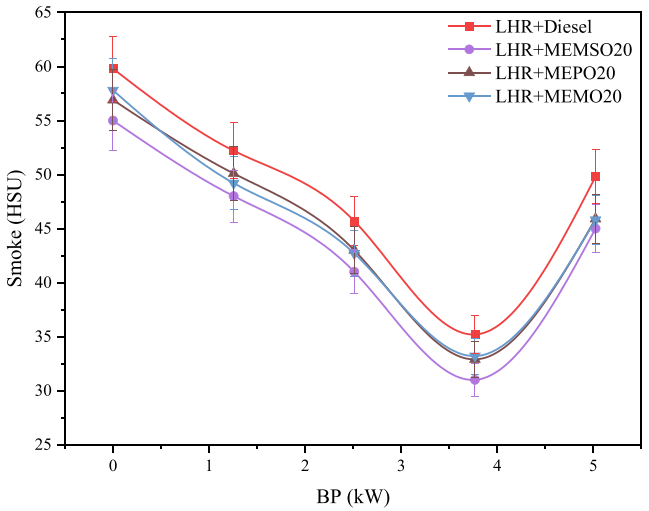

Figure 21. Deviation of smoke vs BP for 20% blends in the LHR engine.

seen from the figure that diesel fuel showed higher smoke emissions at all loads because the aromatic content in fuel leads to incomplete combustion.

5.3. Different Proportions of Antioxidant Additive with Diesel. It is seen from the previous experiments that the performance is increased considerably and other emissions are significantly reduced except NOx emission. The NOx emission is drastically increased because of the excess oxygen in the biodiesel and thermal barrier coating, creating a high combustion chamber temperature. This causes restrictions to have biodiesel as fuel in the CI engine.[32] Therefore, in the present investigation, LA has been chosen as an additive and is added with diesel in different proportions, such as 50, 100, 150, and 200 mg. Experiments are conducted in a conventional engine to find the optimum proportion of additives. The observations are made from the performance and emission parameters with different loads. The graphs are plotted for BP with BTE, BSFC, EGT, CO, HC, NOx, and smoke opacity. The effect of L-ascorbic acid on biodiesel in a conventional engine is elaborately given elaborately.

5.3.1. Brake-Specific Fuel Consumption. The deviation of BSFC for BP for different proportions of LA with diesel is shown in Figure 22. The BSFC for the antioxidant additive mixture is higher than that of diesel.[34] This is due to the little excess fuel supplied to compensate for the slight power loss for adding LA to the diesel. Among the different proportions of LA additive, 200 mg showed lower BSFC than others. This may be due to effective combustion at higher proportions of L-ascorbic acid.

5.3.2. Brake Thermal Efficiency. Figure 23 displays the deviation of BTE concerning the boiling point (BP) for various proportions of linear alkylbenzene (LA) with diesel fuel. The figure demonstrates that BTE increases with the load for all fuels. However, it is observed that BTE is slightly lower for all LA proportions compared to pure diesel across all loads. This indicates that the influence of antioxidant additives on the BTE is not significant. The slight decrease in BTE for all LA proportions can be attributed to the fact that the LA additive does not significantly alter the combustion properties of diesel fuel. While antioxidant additives may have other benefits, such as improving fuel stability or reducing oxidative degradation, they do not notably impact BTE in this context. Furthermore,

https://doi.org/10.1021/acsomega.3c02742
ACS Omega 2023, 8, 36686−36699

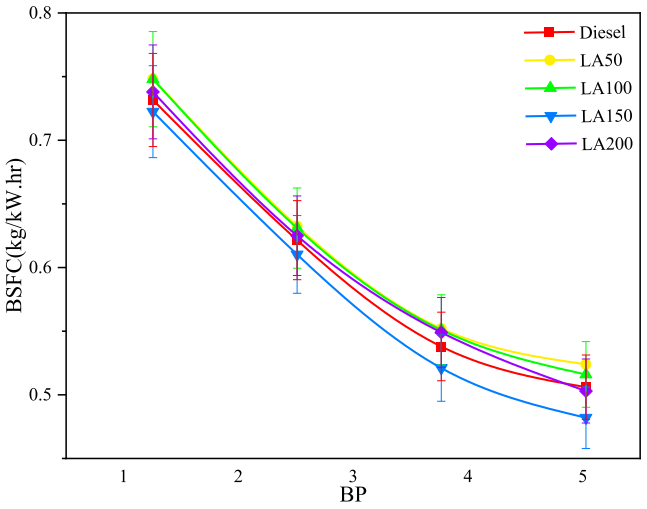

Figure 22. Deviation of BSFC vs BP for different proportions of LA.

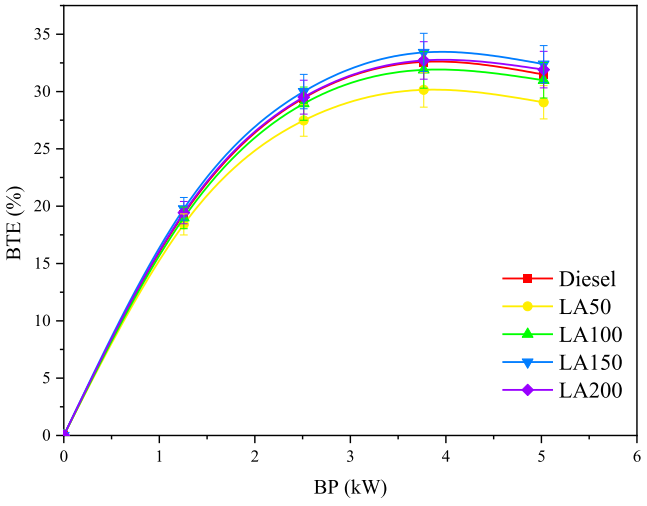

Figure 23. Deviation of BTE vs BP for different proportions of LA.

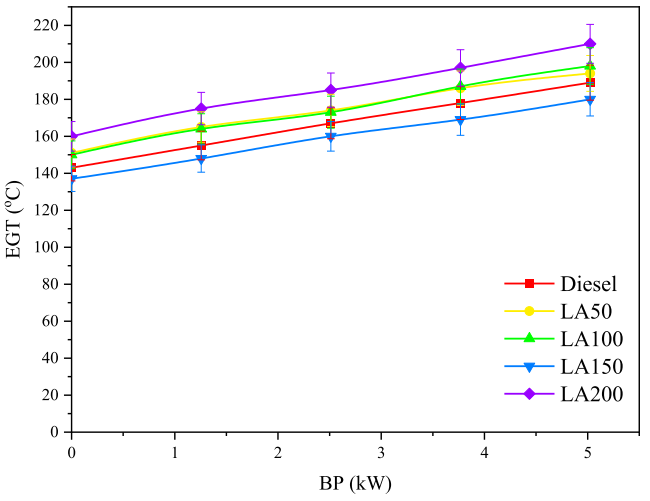

Figure 24. Deviation of EGT vs BP for different proportions of LA.

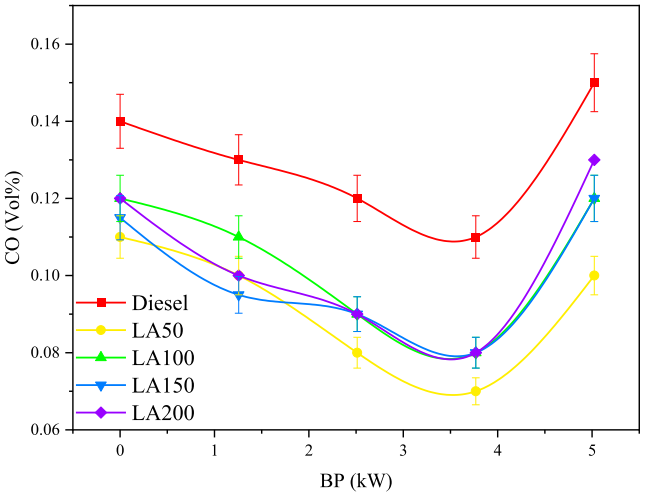

Figure 25. Deviation of CO vs BP for different proportions of LA.

among the different proportions of LA, it was found that the blend containing 200 mg of LA exhibited a higher BTE compared to the other blends. This suggests that this blend achieved a better combustion efficiency or had more favorable properties for higher thermal efficiency. Overall, the findings indicate that adding LA as an antioxidant additive does not significantly affect BTE, as it does not significantly alter the combustion properties of diesel fuel. However, the blend containing 200 mg of LA demonstrated the highest BTE among the LA proportions tested.

5.3.3. Exhaust Gas Temperature. Figure 24 shows the deviation of the EGT concerning BP for different proportions of LA with diesel. It is observed from the figure that the EGT is increased with the load. Among the different fuels, diesel showed higher EGT at all loads. The increase in EGT is due to the lower latent heat of evaporation. It is also observed that 200 mg of LA with diesel has lower EGT among the different proportions. This indicates that effective combustion occurs in the presence of antioxidant additives.

5.3.4. Carbon Monoxide Emission. The deviation of CO concerning BP for different proportions of LA with diesel and diesel is shown in Figure 25. The CO emissions for all fuels decrease with an increase in load. It is also seen that diesel has higher CO emissions, and LA 200 mg showed lower CO emissions at all loads.[35] This is due to the oxidation of CO directly related to the amount of OH radical present in the reaction, and it is high for antioxidants, which contain OH radicals. It is found that the antioxidant additive reduced considerably the CO emission at all loads.

5.3.5. Hydrocarbon Emission. The deviation of the HC for BP for different proportions of LA with diesel is shown in Figure 26. The HC emission is lower for all LA proportions than diesel without additives. It has been found that among various fuels, diesel showed higher HC emission, and LA 200 mg showed lower HC emission at all loads.[36] LA is a reducing agent, which reduces the number of functional groups present in diesel. This leads to a significant reduction of HC emission for all proportions of LA.

5.3.6. Oxides of Nitrogen Emission. The deviation of NOx concerning BP for different proportions of LA with diesel is shown in Figure 27. It is seen from the figure that NOx emissions increase with load for all blends. The addition of LA to the diesel decreases the NOx emission compared with that of diesel. The NOx emission for LA200 mg is lower than that of other antioxidant additive proportions and diesel at all loads. The decrease in NOx emissions is due to the reduction in the formation of free radicals by LA. Further, the NOx decreases

https://doi.org/10.1021/acsomega.3c02742
ACS Omega 2023, 8, 36686−36699

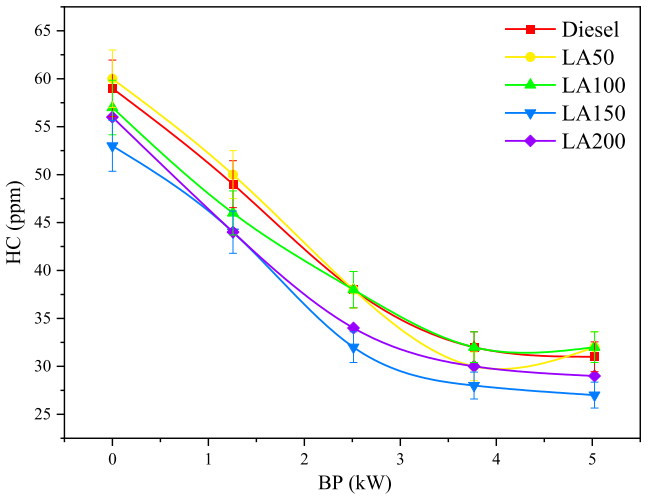

Figure 26. Deviation of HC vs BP for different proportions of LA.

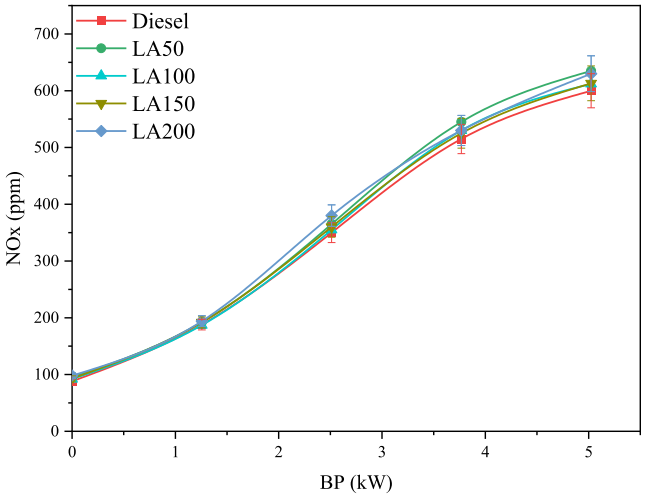

Figure 27. Deviation of NOx vs BP for different proportions of LA.

with an increase in the proportions of LA. This may be due to more free radical formation at higher proportions of the additive.

5.3.7. Smoke Opacity. The deviation of the smoke opacity concerning BP for different proportions of LA with diesel is shown in Figure 28. It is found that smoke emission increases with load for all loads. Among the different fuels, diesel had the highest smoke opacity, and LA 200 mg had the lowest smoke opacity at all loads. This is because effective combustion may happen in the presence of LA.[37] It is also found that the amount of smoke opacity decreases considerably when the proportions.

5.4. Combustion Analysis of B20 Biodiesel with LA in LHR Engine. *5.4.1. Cylinder Pressure.* Figure 29 shows the deviation of cylinder pressure with crank angle for B20 biodiesels with an LA in a LHR engine. It has been found from the graph that MEMSO20 showed a lower cylinder pressure than that of others. This is due to the higher heating value and higher density of MEMSO biodiesel. Further, the MEMSO has better combustion in the presence of additive and thermal barrier coating. It is evident that among the three B20 biodiesels, MEMSO has better combustion than others.

5.4.2. Heat Release Rate. The deviation of the HRR versus crank angle for B20 biodiesels with LA in LHR engines is

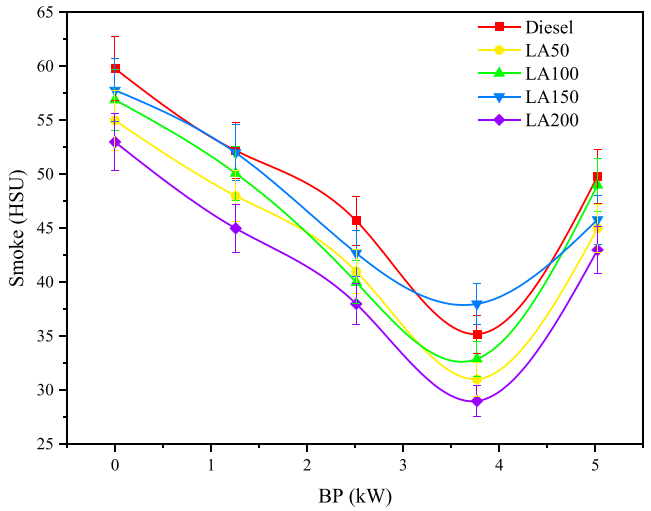

Figure 28. Deviation of smoke opacity vs BP for different proportions of LA.

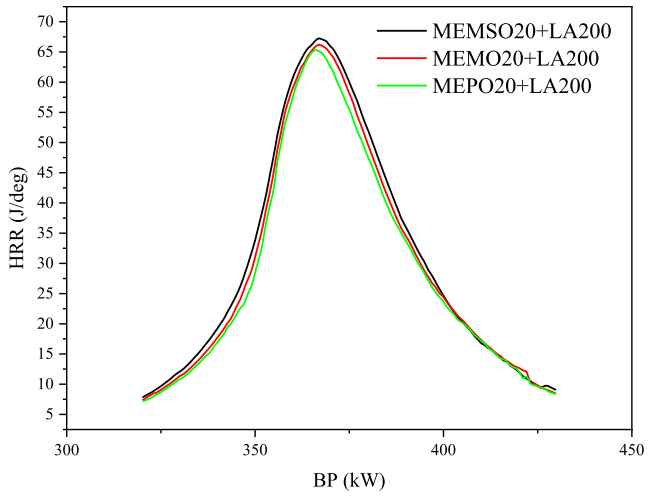

Figure 29. Deviation of cylinder pressure vs crank angle for B20 biodiesels with LA in LHR engine.

illustrated in Figure 30. The figure demonstrates that the HRR of MEMSO20 (a specific biodiesel blend) is higher than that of other blends. This disparity can be attributed to the shorter ID of MEMSO20, resulting in a decrease in the cylinder pressure. Several factors contribute to the higher HRR observed in MEMSO20. First, the shorter ID of MEMSO20 allows for a more rapid and efficient combustion process, leading to a higher HRR.[38] Second, a thermal barrier coating on engine components can enhance the combustion efficiency by reducing heat loss and promoting better heat transfer to the working fluid. Additionally, using additives in the fuel blend can further optimize combustion characteristics, increasing the HRR. Finally, excess oxygen in the fuel mixture can contribute to complete combustion, leading to higher heat release. Factors, including the shorter ID, thermal barrier coating, additives, and excess oxygen content in the fuel, contribute to the higher HRR observed in MEMSO20 than other biodiesel blends.

5.4.3. Ignition Delay. Figure 31 illustrates the deviation between the ID and the BP for B20 biodiesel with LA in a LHR engine. The figure indicates that at maximum load, the ID for 100% load is 6 °CA, which is 4 °CA lower than that of

https://doi.org/10.1021/acsomega.3c02742
ACS Omega 2023, 8, 36686−36699

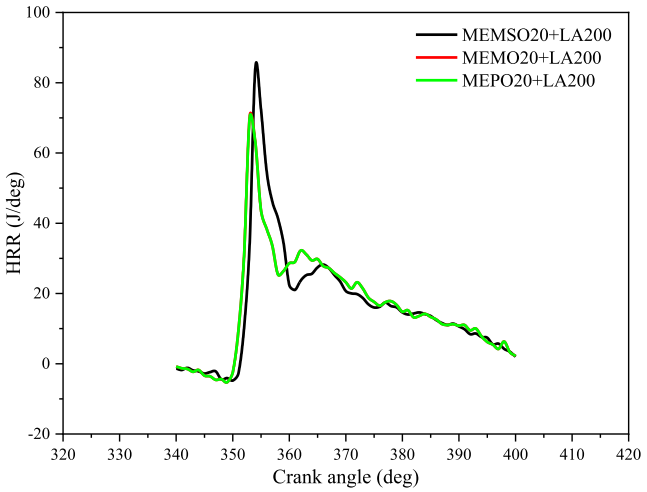

Figure 30. Deviation of HRR vs crank angle for B20 biodiesels with LA in the LHR engine.

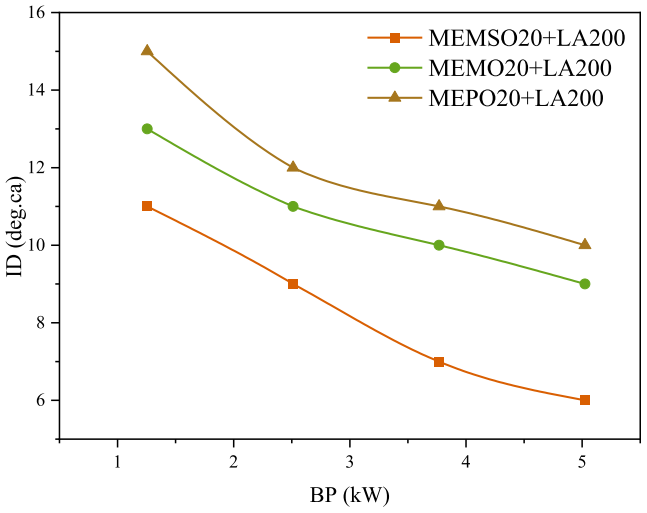

Figure 31. Deviation of ID vs BP for B20 biodiesels with LA in the LHR engine.

MEPO biodiesel. This discrepancy can be attributed to the superior fuel properties of MEMSO biodiesel compared to other biodiesels. Several reasons can explain the exceptional performance of MEMSO biodiesel in terms of ID. First, MEMSO exhibits improved ignition quality, particularly at higher temperatures, which allows for a more efficient and rapid combustion process.[39] This results in a shorter ID compared with other biodiesel blends. Second, the presence of additives in MEMSO biodiesel can further enhance the ignition quality and promote better combustion characteristics, reducing ID. Additionally, the excess oxygen content in the fuel mixture plays a vital role in shortening the ID. Excess oxygen provides a more favorable environment for combustion, facilitating the quick initiation and propagation of the flame front and thereby reducing the ID. Taken together, the superior fuel properties of MEMSO biodiesel, including improved ignition quality at higher temperatures, the presence of additives, and the excess oxygen content in the fuel, contribute to the lowest ID[40−42] observed at all loads in Figure 31.

6. CONCLUSIONS

Different proportions of biodiesel blends (MEMSO, MEPO, and MEMO) exhibit higher BSFC than diesel fuel due to high viscosity and volatility, resulting in poor atomization and mixture formation.

- 100% biodiesel blends demonstrate higher BSFC than 20% biodiesel blends due to their lower heating value, requiring excess fuel to maintain the same power output.
- Diesel fuel outperforms biodiesel blends in BTE in all load conditions due to its higher calorific value and lower density.
- Among the biodiesel blends, MEMSO20 exhibits higher BTE but still lower than diesel due to comparable properties like calorific value, cetane number, and density.
- EGT increases with the proportion of biodiesel blends in all loads. MEPO100 has higher EGT due to its lower calorific value and higher density, resulting in incomplete combustion.
- MEMSO20 demonstrates lower EGT than other blends but slightly higher than diesel due to its excess oxygen content, higher calorific value, and lower density.
- Carbon monoxide (CO) emissions are lower in all biodiesel blends, particularly MEMSO20, than diesel in all load conditions, indicating complete combustion and improved efficiency.
- Hydrocarbon (HC) emissions are lower in MEMSO20 than in other blends and diesel fuel at all loads, while diesel exhibits higher HC emissions due to a lack of oxygen and poor atomization.
- Nitrogen oxide (NOx) emissions are higher in biodiesel blends than diesel fuel in all loads due to the higher combustion temperature and the presence of oxygen. MEMSO demonstrates lower NOx emissions compared to other blends.
- Smoke opacity is lower in MEMSO20 at all loads than in other blends and diesel fuels due to a higher heating value and excess oxygen. MEPO100 shows higher smoke opacity in comparison due to its lower heating value and cetane number. Diesel fuel has higher smoke opacity due to aromatic compounds.
- In the case of using a 20% blend of biodiesel in a LHR engine, MEMSO20 demonstrates better performance than other blends. Still, biodiesel blends overall have lower performance than diesel due to lower calorific values and higher densities.
- Adding an antioxidant additive like L-ascorbic acid (LA) to diesel fuel does not significantly affect BTE. LA blends have higher BSFC than diesel fuel due to a slight power loss. LA blend with 200 mg exhibits lower BSFC, suggesting more effective combustion.

Experimental findings indicate challenges with biodiesel blends with higher BSFC and emissions, particularly NOx. Specific blend proportions, such as MEMSO20, show potential for improved performance and reduced emissions. Adding antioxidant additives such as LA may offer benefits such as improved fuel stability. Further research and optimization are required to enhance performance.

https://doi.org/10.1021/acsomega.3c02742
ACS Omega 2023, 8, 36686−36699

AUTHOR INFORMATION

Corresponding Authors

Elumalai Perumal Venkatesan − *Department of Mechanical Engineering, Aditya Engineering College, Surampalem 533437, India;* orcid.org/0000-0002-7536-8200; Email: elumalaimech89@gmail.com

Silambarasan Rajendran − *Department of Mechanical Engineering, Annapoorana Engineering College, Salem, Tamil Nadu 636308, India;* orcid.org/0000-0003-4017-5940; Email: simbu2explore@gmail.com

Authors

Manickam Murugan − *Department of Mechanical Engineering, Vivekannandha College of Engineering for Woman, Tiruchengode, Namakkal 637205, India*

Sreenivasa Reddy Medapati − *Department of Mechanical Engineering, Aditya Engineering College, Surampalem 533437, India*

Keerty Venkata Sri Ramachandra Murthy − *Department of Electrical and Electronic Engineering, Aditya Engineering College, Surampalem 533437, India*

Mamdooh Alwetaishi − *Department of Civil Engineering, College of Engineering, Taif University, Taif 21944, Saudi Arabia*

Sher Afghan Khan − *Department of Mechanical Engineering, International Islamic University Malaysia, Kuala Lumpur, Wilayah Persekutuan 53100, Malaysia*

Chanduveetil Ahamed Saleel − *Department of Mechanical Engineering, College of Engineering, King Khalid University, Abha 61421, Saudi Arabia*

Complete contact information is available at: https://pubs.acs.org/10.1021/acsomega.3c02742

Notes

The authors declare no competing financial interest.

ACKNOWLEDGMENTS

The authors extend their appreciation to the Deanship of Scientific Research at King Khalid University for funding this work through the large group Research Project under grant number RGP 2/567/44.

NOMENCLATURE DESCRIPTION

CI	compression ignition
BSFC	brake-specific fuel consumption
BTE	brake thermal efficiency
MEMSO	methyl ester mango seed oil
CO	carbon monoxide
HC	hydrocarbon
MOEE	mahua oil ethyl ester
DI	direct injection
NOx	nitrogen oxides
TBC	thermal barrier coating
LHR	low heat rejection
EGT	exhaust gas temperature
SFC	specific fuel consumption
PME	pongamia methyl ester
DEA	diethyl amine
PHC	pyridoxine hydrochloride
TBHQ	*tert* butyl hydroquinone
NPPD	*N*-phenyl-1,4-phenylenediamine
EHN	2-ethylhexyl nitrate
DPPD	*N*,*N*′-diphenyl-1,4-phenylenediamine
NPPD	*N*-phenyl-1,4-phenylenediamine
BHT	butylated hydroxytoluene
PPDA	*p*-phenylenediamine
EDA	ethylenediamine
NO	nitric oxide
MEMO	mahua methyl ester
MEPO	pongamia methyl ester
ASTM	American Society for Testing and Materials
B100	100% biodiesel
MEMSO	methyl ester mango seed oil

REFERENCES

(1) Ebrahimian, E.; Denayer, J. F. M.; Aghbashlo, M.; Tabatabaei, M.; Karimi, K. Biomethane and Biodiesel Production from Sunflower Crop: A Biorefinery Perspective. *Renewable Energy* **2022**, *200*, 1352−1361.

(2) Elgharbawy, A. S.; Ali, R. M. Techno-Economic Assessment of the Biodiesel Production Using Natural Minerals Rocks as a Heterogeneous Catalyst via Conventional and Ultrasonic Techniques. *Renewable Energy* **2022**, *191*, 161−175.

(3) Mawlid, O. A.; Abdelhady, H. H.; El-Deab, M. S. Boosted Biodiesel Production from Waste Cooking Oil Using Novel SrO/MgFe2O4Magnetic Nanocatalyst at Low Temperature: Optimization Process. *Energy Convers. Manag.* **2022**, *273*, 116435.

(4) Ashfaque Ahmed, S.; Soudagar, M. E. M.; Rahamathullah, I.; Sadhik Basha, J.; Yunus Khan, T. M.; Javed, S.; Elfasakhany, A.; Kalam, M. A. Investigation of Ternary Blends of Animal Fat Biodiesel-Diethyl Ether-Diesel Fuel on CMFIS-CI Engine Characteristics. *Fuel* **2023**, *332*, 126200.

(5) Saravanan, A.; Karishma, S.; Senthil Kumar, P.; Jayasree, R. Process Optimization and Kinetic Studies for the Production of Biodiesel from Artocarpus Heterophyllus Oil Using Modified Mixed Quail Waste Catalyst. *Fuel* **2022**, *330*, 125644.

(6) Yaashikaa, P. R.; Keerthana Devi, M.; Senthil Kumar, P.; Pandian, E. A review on biodiesel production by algal biomass: Outlook on lifecycle assessment and techno-economic analysis. *Fuel* **2022**, *324*, 124774.

(7) Nayab, R.; Imran, M.; Ramzan, M.; Tariq, M.; Taj, M. B.; Akhtar, M. N.; Iqbal, H. M. N. Sustainable Biodiesel Production via Catalytic and Non-Catalytic Transesterification of Feedstock Materials - A Review. *Fuel* **2022**, *328*, 125254.

(8) Wu, G.; Wang, X.; Abubakar, S.; Li, Y. A Skeletal Mechanism for Biodiesel-Dimethyl Ether Combustion in Engines. *Fuel* **2022**, *325*, 124834.

(9) Rajendran, N.; Kang, D.; Han, J.; Gurunathan, B. Process Optimization, Economic and Environmental Analysis of Biodiesel Production from Food Waste Using a Citrus Fruit Peel Biochar Catalyst. *J. Clean. Prod.* **2022**, *365*, 132712.

(10) Yahya, M.; Dutta, A.; Bouri, E.; Wadström, C.; Uddin, G. S. Dependence Structure between the International Crude Oil Market and the European Markets of Biodiesel and Rapeseed Oil. *Renewable Energy* **2022**, *197*, 594−605.

(11) Zhu, X.; Liu, S.; Wang, Z.; Zhang, Q.; Liu, H. Study of the Effect of Methanol/Biodiesel Fuel Mixtures on the Generation of Soot Particles and Their Oxidation Reactivity. *Fuel* **2023**, *341*, 127632.

(12) Maroušek, J.; Strunecký, O.; Bartoš, V.; Vochozka, M. Revisiting Competitiveness of Hydrogen and Algae Biodiesel. *Fuel* **2022**, *328*, 125317.

(13) Szulczyk, K. R.; Badeeb, R. A. Nontraditional Sources for Biodiesel Production in Malaysia: The Economic Evaluation of Hemp, Jatropha, and Kenaf Biodiesel. *Renewable Energy* **2022**, *192*, 759−768.

(14) Zhang, W.; Wang, C.; Luo, B.; He, P.; Zhang, L.; Wu, G. Efficient and Economic Transesterification of Waste Cooking Soybean Oil to Biodiesel Catalyzed by Outer Surface of ZSM-22

Supported Different Mo Catalyst. *Biomass Bioenergy* **2022**, *167*, 106646.
(15) Iyyappan, J.; Jayamuthunagai, J.; Bharathiraja, B.; Saravanaraj, A.; Praveen Kumar, R.; Balraj, S. Production of Biodiesel from Caulerpa Racemosa Oil Using Recombinant Pichia Pastoris Whole Cell Biocatalyst with Double Displayed over Expression of Candida Antartica Lipase. *Bioresour. Technol.* **2022**, *363*, 127893.
(16) Zhang, X.; Li, N.; Wei, Z.; Dai, B.; Han, S. Synthesis and Evaluation of Bifunctional Polymeric Agent for Improving Cold Flow Properties and Oxidation Stability of Diesel-Biodiesel Blends. *Renewable Energy* **2022**, *196*, 737−748.
(17) Sharma, P.; Sharma, A. K.; Balakrishnan, D.; Manivannan, A.; Chia, W. Y.; Awasthi, M. K.; Show, P. L. Model-Prediction and Optimization of the Performance of a Biodiesel - Producer Gas Powered Dual-Fuel Engine. *Fuel* **2023**, *348*, 128405.
(18) Gohar Khan, S.; Hassan, M.; Anwar, M.; Zeshan; Masood Khan, U.; Zhao, C. Mussel Shell Based CaO Nano-Catalyst Doped with Praseodymium to Enhance Biodiesel Production from Castor Oil. *Fuel* **2022**, *330*, 125480.
(19) Uyumaz, A. Experimental Evaluation of Linseed Oil Biodiesel/Diesel Fuel Blends on Combustion, Performance and Emission Characteristics in a DI Diesel Engine. *Fuel* **2020**, *267*, 117150.
(20) Yesilyurt, M. K. A Detailed Investigation on the Performance, Combustion, and Exhaust Emission Characteristics of a Diesel Engine Running on the Blend of Diesel Fuel, Biodiesel and 1-Heptanol (C7 Alcohol) as a next-Generation Higher Alcohol. *Fuel* **2020**, *275*, 117893.
(21) Longati, A. A.; Campani, G.; Furlan, F. F.; Giordano, R. d. C.; Miranda, E. A. Microbial Oil and Biodiesel Production in an Integrated Sugarcane Biorefinery: Techno-Economic and Life Cycle Assessment. *J. Clean. Prod.* **2022**, *379*, 134487.
(22) Sharma, V.; Kalam Hossain, A.; Ahmed, A.; Rezk, A. Study on Using Graphene and Graphite Nanoparticles as Fuel Additives in Waste Cooking Oil Biodiesel. *Fuel* **2022**, *328*, 125270.
(23) Mahmoud, A. H.; Hussein, M. Y.; Ibrahim, H. M.; Hanafy, M. H.; Salah, S. M.; El-Bassiony, G. M.; Abdelfattah, E. A. Mixed Microalgae-Food Waste Cake for Feeding of Hermetia Illucens Larvae in Characterizing the Produced Biodiesel. *Biomass Bioenergy* **2022**, *165*, 106586.
(24) Chen, Y.; Long, F.; Huang, Q.; Wang, K.; Jiang, J.; Chen, J.; Xu, J.; Nie, X. Biodiesel Production from Rhodosporidium Toruloides by Acidic Ionic Liquids Catalyzed Hydrothermal Liquefaction. *Bioresour. Technol.* **2022**, *364*, 128038.
(25) Gupta, R.; McRoberts, R.; Yu, Z.; Smith, C.; Sloan, W.; You, S. Life Cycle Assessment of Biodiesel Production from Rapeseed Oil: Influence of Process Parameters and Scale. *Bioresour. Technol.* **2022**, *360*, 127532.
(26) Wahyono, Y.; Hadiyanto, H.; Gheewala, S. H.; Budihardjo, M. A.; Adiansyah, J. S. Evaluating the Environmental Impacts of the Multi-Feedstock Biodiesel Production Process in Indonesia Using Life Cycle Assessment (LCA). *Energy Convers. Manag.* **2022**, *266*, 115832.
(27) Manimaran, R.; Venkatesan, M.; Tharun Kumar, K. Optimization of Okra (Abelmoschus Esculentus) Biodiesel Production Using RSM Technique Coupled with GA: Addressing Its Performance and Emission Characteristics. *J. Clean. Prod.* **2022**, *380*, 134870.
(28) Zhang, X.; Li, N.; Wei, Z.; Dai, B.; Lin, H.; Han, S. Enhanced the Effects on Improving the Cold Flow Properties and Oxidative Stability of Diesel-Biodiesel Blends by Grafting Antioxidant on PMA Type Pour Point Depressant. *Fuel Process. Technol.* **2022**, *238*, 107483.
(29) Song, S. S.; Tian, B. C.; Chen, H.; Chi, Z.; Liu, G. L.; Chi, Z. M. Transformation of Corncob-Derived Xylose into Intracellular Lipid by Engineered Strain of Aureobasidium Melanogenum P10 for Biodiesel Production. *Renewable Energy* **2022**, *200*, 1211−1222.
(30) Torkzaban, S.; Feyzi, M.; norouzi, L. A Novel Robust CaO/ZnFe2O4 Hollow Magnetic Microspheres Heterogenous Catalyst for Synthesis Biodiesel from Waste Frying Sunflower Oil. *Renewable Energy* **2022**, *200*, 996−1007.
(31) Karimi, S.; Saidi, M. Biodiesel Production from Azadirachta India-Derived Oil by Electrolysis Technique: Process Optimization Using Response Surface Methodology (RSM). *Fuel Process. Technol.* **2022**, *234*, 107337.
(32) Tamjidi, S.; Kamyab Moghadas, B.; Esmaeili, H. Ultrasound-Assisted Biodiesel Generation from Waste Edible Oil Using CoFe2O4@GO as a Superior and Reclaimable Nanocatalyst: Optimization of Two-Step Transesterification by RSM. *Fuel* **2022**, *327*, 125170.
(33) Kukana, R.; Jakhar, O. P. Effect of Ternary Blends Diesel/n-Propanol/Composite Biodiesel on Diesel Engine Operating Parameters. *Energy* **2022**, *260*, 124970.
(34) Han, K.; Lin, Q.; Liu, M.; Meng, K.; Ni, Z.; Liu, Y.; Tian, J.; Qiu, Z. Experimental Study on the Micro-Explosion Characteristics of Biodiesel/1-Pentanol and Biodiesel/Methanol Blended Droplets. *Renewable Energy* **2022**, *196*, 261−277.
(35) Aghel, B.; Gouran, A.; Parandi, E.; Jumeh, B. H.; Nodeh, H. R. Production of Biodiesel from High Acidity Waste Cooking Oil Using Nano GO@MgO Catalyst in a Microreactor. *Renewable Energy* **2022**, *200*, 294−302.
(36) Li, R.; Wang, S.; Zhang, H.; Li, F.; Sui, M. Synthesis, Antioxidant Properties, and Oil Solubility of a Novel Ionic Liquid [UIM0Y2] [C6H2(OH)3COO] in Biodiesel. *Renewable Energy* **2022**, *197*, 545−551.
(37) Jayaraman, J.; Dawn, S. S.; Appavu, P.; Mariadhas, A.; Joy, N.; Alshgari, R. A.; Karami, A. M.; Huong, P. T.; Rajasimmam, M.; Kumar, J. A. Production of Biodiesel from Waste Cooking Oil Utilizing Zinc Oxide Nanoparticles Combined with Tungsto Phosphoric Acid as a Catalyst and Its Performance on a CI Engine. *Fuel* **2022**, *329*, 125411.
(38) Zhang, Y.; Lou, D.; Tan, P.; Hu, Z.; Fang, L. Effects of Waste-Cooking-Oil Biodiesel Blends on Diesel Vehicle Emissions and Their Reducing Characteristics with Exhaust after-Treatment System. *J. Clean. Prod.* **2022**, *381*, 135190.
(39) Gowrishankar, S.; Krishnasamy, A. Novel Surfactants for Stable Biodiesel-Water Emulsions to Improve Performance and Reduce Exhaust Emissions of a Light-Duty Diesel Engine. *Fuel* **2022**, *330*, 125562.
(40) Elumalai, P. V.; Parthasarathy, M.; Murugan, M.; Saravanan, A.; Sivakandhan, C. Effect of Cerium Oxide Nanoparticles to Improve the Combustion Characteristics of Palm Oil Nano Water Emulsion Using Low Heat Rejection Engine. *Int. J. Green Energy* **2021**, *18*, 1482−1496.
(41) Sivalingam, A.; Perumal Venkatesan, E.; Roberts, K. L.; Asif, M. Potential Effect of Lemon Peel Oil with Novel Eco-Friendly and Biodegradable Emulsion in Un-Modified Diesel Engine. *ACS Omega* **2023**, *8* (21), 18566−18581.
(42) Ramalingam, K.; Vellaiyan, S.; Venkatesan, E. P.; Khan, S. A.; Mahmoud, Z.; Saleel, C. A. Challenges and Opportunities of Low Viscous Biofuel−A Prospective Review. *ACS Omega* **2023**, *8* (19), 16545−16560.

https://doi.org/10.1021/acsomega.3c02742
ACS Omega 2023, 8, 36686−36699